Nuclear magnetization distribution radii determined by hyperfine transitions in the 1*s* level of H-like ions $^{185}Re^{74+}$ and $^{187}Re^{74+}$

J. R. Crespo López-Urrutia, P. Beiersdorfer, and K. Widmann
Lawrence Livermore National Laboratory, Livermore, California 94550

B. B. Birkett
Department of Physics, University of California at Berkeley, Berkeley, California 94720

A.-M. Mårtensson-Pendrill and M. G. H. Gustavsson
Department of Physics, Göteborg University and Chalmers University of Technology, SE-412 96, Sweden
(Received 12 August 1997)

The $F=3$ to $F=2$ hyperfine transitions in the 1*s* ground state of the two isotopes $^{185}Re^{74+}$ and $^{187}Re^{74+}$ were measured to be (4560.5±3) Å and (4516.9±3) Å, respectively, using emission spectroscopy in an electron beam ion trap. After applying appropriate corrections for the nuclear charge distribution and QED effects, a Bohr-Weisskopf effect of $\varepsilon=2.23(9)\%$ and 2.30(9)% are found for ^{185}Re and ^{187}Re, respectively. This value is almost twice that of a previous theoretical estimate, and indicates a distribution of the nuclear magnetization far more extended than that of the nuclear charge. A radius of the magnetization distribution of $\langle r_m^2\rangle^{1/2}=7.57(32)$ fm and $\langle r_m^2\rangle^{1/2}=7.69(32)$ fm for ^{185}Re and ^{187}Re, respectively, is inferred from the data. These radii are larger than the nuclear charge distribution radius $[\langle r_c^2\rangle^{1/2}=5.39(1)$ fm] for both isotopes by factors 1.40(6) and 1.43(6), respectively. We find that the Bohr-Weisskopf effect in H-like ions is a sensitive probe of nuclear magnetization distribution, especially for cases where the charge distribution and magnetic moments are accurately known. [S1050-2947(98)02002-2]

PACS number(s): 32.10.Fn, 32.30.Jc, 31.30.Gs, 21.10.Gv

I. INTRODUCTION

The discovery of the hyperfine structure (hfs) established a bridge between nuclear and atomic physics that has served as a tool for the scrutiny of nuclear properties and basic physical principles. The derivation of the value of the nuclear magnetic moment by Fermi [1] from the hyperfine structure of the Cs and Na (measured in the optical spectra of those elements by Jackson [2] and Schüler [3]) is one example. Other examples are the nuclear charge distribution effect postulated by Breit and Rosenthal [4], and the nuclear magnetization distribution (NMD) postulated by Bohr and Weisskopf [5,6], to explain an isotopic dependence in the ratio between hyperfine structures and nuclear *g* factors, known as the ''hyperfine anomaly.'' The influence of the nucleus on the electronic energy levels and the associated line emission can be precisely measured by an assortment of accurate, high resolution optical, laser, and microwave tools. The results have challenged theory and have stimulated different branches of atomic and nuclear physics [7,8].

The precision of current NMD data has not been sufficient to distinguish among nuclear models. The lack of such data affects several problems in this region of overlap between atomic and nuclear physics. The first is the interpretation of atomic parity nonconservation (PNC) experiments, which is limited by the uncertainty in the distribution of neutrons in the nucleus [9]. The second is the fact that the nuclear anapole moment recently observed by Wood *et al.* [10] can arise from several different effects and a good understanding of the nuclear wave function is essential for the analysis of experimental data [11–17]. A proton electric dipole moment (EDM), which would violate parity (P) and time (T) reversal invariance, could lead to an observable nuclear EDM if charge and electric dipole distributions differ [18]. A nuclear EDM, like the magnetic moment, can be expected to arise mainly from the valence nucleon, and information about the NMD would thus be valuable for the interpretation of experiments searching for an EDM [19–22].

The principal aim of this paper's work is to provide experimental data that can be used to infer the magnetic structure of the nucleus. We believe that the method presented here is more appropriate to determine the nuclear magnetization distribution than any of the techniques currently in use, as we will show below.

The main tool for studying NMD has been measuring γ rays emitted by muonic atoms (see, e.g., Büttgenbach [8]). For high Z nuclei, the Bohr-Weisskopf effect reduces the separation of the hyperfine level in the 1*s* state by 50%. However, while this effect is on the order of a few keV, it has to be extracted from γ-ray transitions corresponding either to muonic or nuclear transitions, which have energies of several MeV and large experimental uncertainties. The initial cascade, when the captured muon relaxes from high n levels ($n\approx14$) mainly by ejection of Auger electrons, leaves the originally neutral atom in an ionized state; this causes small electronic screening effects even in the 1*s* muon. The muon also strongly polarizes the nuclear charge distribution, creating additional uncertainties. Ideally, the Bohr-Weisskopf effect is determined directly from the hyperfine transition within the muonic 1*s* level. This transition, however, cannot be directly observed for the following reasons:

(a) The upper hyperfine level may relax by emission of an Auger ($M1$) electron (extrapolating the rates given by Winston [23] to $Z\approx75$) in a picosecond time scale. This is more

than three orders of magnitude faster than the radiative $M1$ hyperfine transition.

(b) The weak interaction with nuclear matter captures the $1s$ muon at rates of 10^8 s^{-1}.

(c) The lifetime of the muon (2.2 μs) also quenches the upper hyperfine F level, although less significantly than the other two effects for high-Z elements.

Hence, all of these processes happen well before the $1s$ hyperfine transition can take place and make its observation close to impossible. Due to these limitations, the study of muonic atoms has delivered results for the Bohr-Weisskopf effect with uncertainties on the order of several percent [24], which is not sufficient to distinguish among different nuclear models, as pointed out in a review of the magnetic hyperfine anomalies by Büttgenbach [8]. The usefulness of other exotic atoms containing hadrons for the study of the Bohr-Weisskopf (BW) effect is similarly limited, especially by the strong nuclear forces present when the wave function of those particles and the nucleus overlap, which quench all atomic states with a strong magnetic interaction between the nuclear magnetization distribution and the orbiting particle.

Despite the remarkable accuracy achieved by laser spectroscopic techniques, measurements of neutral atoms involving valence electrons are not particularly suitable for determining the size of the BW effect either, since they need complex atomic structure calculations for the interpretation to take into account many-electron correlations. Measurements of hyperfine anomalies can, however, give information about differences in the NMD for different isotopes of the same element.

Nuclear size effects are more pronounced on the $1s$ electrons, which are also less sensitive to correlation effects. To measure them on an absolute scale with x-ray transitions involving a hole in the K shell requires a resolution in the x-ray region still beyond the experimental possibilities; only isotopic variations have been measured (see, e.g., [25]).

In contrast to the complexity of muonic or neutral electronic atoms, the simplicity of one-electron ions in the hydrogenic isoelectronic sequence offers great advantages for the theoretical modeling and therefore for the interpretation of experimental data. All contributions related to the presence of a single electron are theoretically well understood. The experimental precision can be very high, as seen in the hydrogen atom, where the hfs splitting of the ground state has become one of the most accurately measured physical quantities [26]. The spontaneous $1s$ hyperfine transition in H, D, and He^+ has been observed in astrophysical sources, but few laboratory measurements have been carried out (H, D, T, He^+) due to the extremely long lifetime of the upper hyperfine levels in neutrals and low-charged ions [7]. The hfs of H-like ions had until recently only been accessible to experimental research in the cases He^+ and Li^{2+}.

There is a large interest in expanding this field of research into higher-Z elements. The sensitivity of the $1s$ electrons to nuclear and QED effects is greatly enhanced by the spatial overlap of their wave functions with the nucleus, which lets the total hfs splitting scale with approximately Z^3. The $1s$ hyperfine transition in hydrogen has a wavelength of 21 cm. At around $Z>65$, the transition between the two F levels of the $1s$ ground state scales into the infrared, visible, and uv region of the electromagnetic spectrum depending on the particular value of the magnetic moment of the nucleus. Such highly charged hydrogenlike ions are now routinely produced and studied using both electron beam ion traps (EBIT) and heavy ion storage rings. Recently, several measurements of the ground-state hyperfine splitting of highly charged ions have been published. Using the GSI storage ring and laser excitation an energy splitting of 5.0840(8) eV between the $F=5$ and $F=4$ states of H-like $^{209}Bi^{82+}$ was obtained [27]. Using a high-energy electron beam ion trap at LLNL (SuperEBIT), 2.1645(6) eV was obtained for the energy difference between the levels $F=4$ and $F=3$ of H-like $^{165}Ho^{66+}$ [28] and 0.821(26) eV for the energy difference between the $F=5$ and $F=4$ states of Li-like Bi^{80+} [29].

In the following we present a measurement of the hyperfine splitting of the $1s$ ground level in H-like rhenium. The measurement is carried out for both naturally occurring isotopes of Re, ^{185}Re, and ^{187}Re. Because the nuclear parameters needed to infer the Bohr-Weisskopf correction factor ε from the value of the hyperfine splitting are known with high accuracy, we use the measurement of Re to determine the nuclear magnetization distribution and infer the magnetization radius. This shows that hyperfine structure measurements in high-Z H-like ions provide a direct window on the magnetic properties of the nucleus, including the neutron distribution, that is not afforded by any other technique currently available.

II. THEORY

Analog to the hydrogen atom, in hydrogenic ions the coupling between the nuclear spin I (if the nucleus has one) and the total electron angular momentum $J=\frac{1}{2}$ splits the ground state in two F levels $F=I+J$, $I-J$. The main term contributing to the separation of the hfs levels of the ground state of a highly charged hydrogenlike ion is linearly dependent on the magnetic moment of the nucleus. The energy difference ΔE between the two neighboring levels with highest F values in a H-like ion is given by Shabaev [30] as

$$\Delta E=\frac{\alpha^4 Z^3}{n^3}\frac{\mu_I}{I}\frac{m_e}{m_p}\frac{(I+j)m_e c^2}{j(j+1)(2l+1)}[A(1-\delta)(1-\varepsilon)+\kappa_{\rm rad}] \tag{1}$$

with the following terms: α, fine-structure constant; Z, nuclear charge; n, the principal quantum number; l and j, the orbital and total angular momentum quantum numbers; μ_L, nuclear magnetic moment; m_e, m_p: electron, proton mass; I, nuclear spin; A, relativistic correction factor; δ, nuclear charge distribution correction; ε, nuclear magnetization distribution (Bohr-Weisskopf) correction; $\kappa_{\rm rad}$, QED radiative corrections.

The QED corrections applied are small because of cancellation effects and can be calculated to an appropriate degree of accuracy by using well established theoretical methods (for the self-energy, see Persson *et al.* [31]; for the vacuum polarization see Schneider *et al.* [32] and also Sunnergren *et al.* [33]). The net QED contribution to the electron energy accounts for a few tenths of one percent of the total energy splitting of the $1s$ level for heavy ions.

Approximate expressions for the relativistic correction factor A, independent of the principal quantum number, were

obtained by Breit [34] and Racah [35] and have been tabulated by Kopfermann [36]. More complete expressions, including the n dependence, are given by Pyykkö *et al.* [37], with results tabulated for Z up to 100. This factor A is of the order 1.2 to 2.8 for high-Z ions.

A. Nuclear charge distribution

Nuclear size effects produce important contributions. To treat those, series expansions of the electronic wave functions close to the nucleus can be obtained analytically for certain nuclear charge distributions, and were utilized already in the early days of hyperfine anomaly studies [5,6,38]. Kopfermann [36] indicated a reduction of the hfs of about 10% for $Z=75$ resulting from finite size effects. Shabaev [30] recently followed again this approach to calculate the hyperfine structure for a number of hydrogenlike systems of experimental interest, using a homogeneous charge distribution.

The shape of an arbitrary nuclear distribution can often be adequately described by the moments $\langle r_c^{2n}\rangle$ of the distribution [39]. The sensitivity to changes in the charge distribution is seen most easily by writing the hyperfine splitting parameter in terms of changes in the moments, $\langle r_c^{2n}\rangle$, of the charge distribution, relative to a reference distribution,

$$\Delta E=\Delta E_0[1+x_2\delta\langle r_c^2\rangle+x_4\delta\langle r_c^4\rangle+x_6\delta\langle r_c^6\rangle]. \tag{2}$$

The Fermi distribution, $\rho_c(r)=\rho_0/(1+e^{(r-c)/a})$, where the charge density $\rho_c(r)$ is given in terms of the parameters c (half-density thickness) and a (skin thickness), is a convenient way to model different nuclear distributions. The calculated hfs splitting can then be written

$$\Delta E=\Delta E_0[1+x_r\delta\langle r_c^2\rangle+x_a\delta a^2] \tag{3}$$

in terms of $\delta\langle r_c^2\rangle$ and δa^2.

B. Nuclear magnetization distribution

The magnetic moment distribution can, to a first approximation, be expected to follow the distribution of the unpaired nucleon(s). By contrast, *all* protons contribute to the charge distribution. We can thus expect the average magnetic radius $\langle r_m^2\rangle$ to be larger than $\langle r_c^2\rangle$ and also to find that the magnetization distribution is more sensitive to perturbations. Investigations of the ''hyperfine anomalies'' for the Tl isotopes showed that the difference in magnetization distribution between ^{203}Tl and ^{205}Tl is about twice as large as the change in the charge distribution [40]. In general the corrections for the distribution of nuclear magnetization can be expressed in terms of a parameter ε in Eq. (1), which relates the hyperfine structure for an ideal point magnetic dipole and a realistic distributed magnetization. Following Shabaev [30] and earlier work [5,6], the effect for an arbitrary nuclear distribution is written in terms of integrals in the form

$$\begin{aligned}\langle\kappa_S\rangle&=4\pi\int_0^\infty\kappa_S(R)w_S(R)R^2dR\\&=a_2\langle R^2\rangle+a_4\langle R^4\rangle+a_6\langle R^6\rangle,\end{aligned}$$

$$\begin{aligned}\langle\kappa_L\rangle&=4\pi\int_0^\infty\kappa_L(R)w_L(R)R^2dR\\&=b_2\langle R^2\rangle+b_4\langle R^4\rangle+b_6\langle R^6\rangle.\end{aligned} \tag{4}$$

In the extreme single particle model, the nuclear magnetic moment is due to a single unpaired nucleon. The values $\langle R^{2n}\rangle$ needed in Eqs. (4) are then simply given by the corresponding expectation values for the unpaired nucleon. In general, the nuclear wave function is more complex. Taking many-body effects into account leads to three different sets of ''effective'' $\langle R^{2n}\rangle$ parameters, corresponding to spin, orbital, and spin asymmetry contributions to the magnetic moment. (These parameters are analogous to the contact, orbital, and spin-dipole parameters often used to analyze the electronic part of the hyperfine structure.) In our analysis of experimental results we have, however, not distinguished between these contributions. The total correction due to the nuclear magnetization distribution can then be written as

$$\varepsilon=\alpha_S[\langle\kappa_S\rangle+\zeta(\langle\kappa_S\rangle-\langle\kappa_L\rangle)]+\alpha_L\langle\kappa_L\rangle, \tag{5}$$

where

$$\alpha_S=\frac{g_S}{g_I}\,\frac{g_I-g_L}{g_S-g_L} \tag{6}$$

and

$$\alpha_L=1-\alpha_S, \tag{7}$$

and the spin asymmetry parameter ζ is given by

$$\zeta=\begin{cases}\dfrac{2I-1}{4(I+1)} & \text{for } I=l+\frac{1}{2}\\[2ex] \dfrac{2I+3}{4I} & \text{for } I=l-\frac{1}{2}\end{cases} \tag{8}$$

in the extreme single particle model [5], where the total nuclear angular momentum is considered to be due to one unpaired nucleon. The spin g factor can then be determined from the relation given by Bohr and Mottelson [41]:

$$\mu=I\left[g_L\pm(g_S-g_L)\,\frac{1}{2l+1}\right]\quad\text{for } I=l\pm\tfrac{1}{2}, \tag{9}$$

since g_L is commonly set to 1 and 0 for a proton and a neutron, respectively. For the two Re isotopes studied here, we find, by inserting the different magnetic moments in these expressions, $g_s(^{185}\mathrm{Re})=2.374$ and $g_s(^{187}\mathrm{Re})=2.439$, giving $\alpha_s(^{185}\mathrm{Re})=0.372$ and $\alpha_s(^{187}\mathrm{Re})=0.379$.

III. EXPERIMENT

A. Ion production and trapping

The setup of this experiment has been reported in [28]. The production of hydrogenlike rhenium ions in a high-energy electron beam ion trap (SuperEBIT) relies on electron impact ionization. An electron beam of variable energy is axially compressed by a high magnetic field to a radius of 35 μm and creates an electron density of up to 10^{13} e/cm^3. In the electrical field created by the associated space charge,

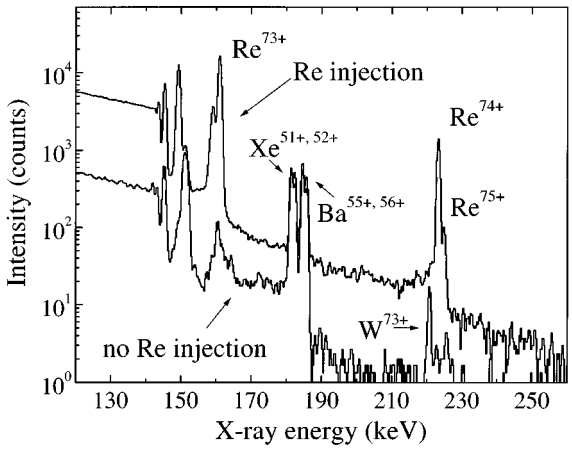

FIG. 1. X-ray spectrum of the trap showing runs with and without Re.

ions experience a force towards the electron beam. A set of three drift tubes defines a potential minimum in the middle drift tube, confining the ions in the vertical direction. The trap is initially loaded by introducing low charge Re ions from a metal vapor vacuum arc (MEVVA) injected into the trap through a beam line also used for ion extraction. The MEVVA used here contained natural Re (37% ^{185}Re, 63% ^{187}Re). The trapped ions are denuded of all electrons having binding energies lower than the electron beam energy by successive electron impact processes during the long trapping cycles (20 s typically in the present measurement).

The ion trap is monitored by a germanium detector to determine the ionic species present and the charge balance. Figure 1 shows part of the x-ray spectrum emitted by the ions in the trap under beam excitation at 141 keV. The region displayed shows the radiative recombination lines (RR), produced when the free, nearly monoenergetic beam electrons are captured by the ions into vacancies in the different shells. The photon energy consists of the sum of the beam energy plus the ionization energy for the vacancy filled by the captured electron. The most prominent line corresponds to radiative recombination into levels with $n=2$ and $j=\frac{1}{2}$, that is, ions belonging to the He-Li-Be-B-C isoelectronic sequences. Spectra taken with and without Re injection are displayed for comparison. When no Re is injected, the trap fills up in few seconds with Ba ions, evaporated from the *e*-gun cathode, and Xe ions from background gas. We estimate the charge balance in the trap from the radiative recombination spectrum by taking into account the radiative recombination cross sections and the detector efficiency as a function of the photon energy. Under the conditions shown, the most abundant species in the trap were the He-like Re^{73+} ion and the Li-like Re^{72+} in roughly the same concentration. Both charge states together comprise approximately 75% of the ion contents of the trap. The concentration of H-like Re^{74+} was around 6%, bare Re^{75+} was estimated at only 0.2%, and the Be-like and other lower charge states made up the rest. At a beam energy of 163 keV and 280 mA beam current, we observed fractions of H-like Re^{74+} near 10%. The energy resolution in those x-ray spectra is degraded by pile-up from the much increased bremsstrahlung of the beam, but they display the same features as Fig. 1.

B. Population of the upper hyperfine level

Two main processes are expected to populate the upper hyperfine level of the H-like ion in our trap. The most important is collisional ionization of He-like ions, where one of the two 1*s* electrons is removed leaving a H-like ion behind with similar probability for population in any of the two hfs states. The second process is radiative recombination of beam electrons with bare ions, also populating both hfs levels nearly evenly. Collisional excitation requiring a spin flip is far less probable than these two mechanisms and can be neglected. With these processes, and taking into account the spectrograph's detection efficiency, the observed photon count rate can be explained. Since the trap reaches a quasi-steady state within a few seconds, the rates for ionization and recombination become the same; therefore, the RR peak of $n=1$ indicates how much H-like Re^{74+} recombines into He-like and at the same time how much He-like is ionized into H-like rhenium. This process, as already mentioned, populates both hyperfine levels statistically. This rate was calculated to be approximately $7\ s^{-1}$ in steady state by a code including rate equations for ionization, recombination, and charge exchange under the given experimental conditions.

C. Detection of optical radiation

We use a prism spectrograph equipped with a cryogenic CCD camera to detect the spontaneous emission from the hyperfine transitions in the H-like ions. Due to the extreme low number of emitting ions (thousands), and the low excitation rate ($<10\ s^{-1}$), great care was necessary to separate the signals on the order of a few tens of photons per hour from much higher levels of background. A cutoff filter (BG38) is used to reduce the near-IR stray light background above 6700 Å. The total detection efficiency of the system, after taking into consideration a solid angle collection efficiency of 7×10^{-4}, is around 2.5×10^{-4}. The thermal and atomic line background are eliminated by subtracting from every spectrum taken with Re ions in the trap another one taken without Re injection. Cosmic rays are detected by the CCD during the long exposure times. Their contribution is largely reduced by an appropriate software discriminator level during the data reduction. To obtain spectra from the two-dimensional images, the pixel counts on the CCD detector are integrated along one dimension.

D. Wavelength calibration

For the calibration of the spectrograph, we use the procedure already described in [28] repeatedly during the experiment. Neutral gases were injected as an atomic beam into the trap; the atoms crossing the electron beam are excited and emit visible radiation characteristic for the element in question. The full visible range can be calibrated with this method with a nonlinear wavelength scale interpolated by a least-squares approximation of a fourth-order polynomial. In a range of 200 Å around the interesting features, approximately 5 He I, 20 Ar I, and Ar II and 15 Kr I and Kr II lines are found. Their measured wavelengths are taken from standard reference books, and have uncertainties around 0.01 Å, making the wavelength calibration error only a fraction of 1 Å. This uncertainty is negligible compared with the statisti-

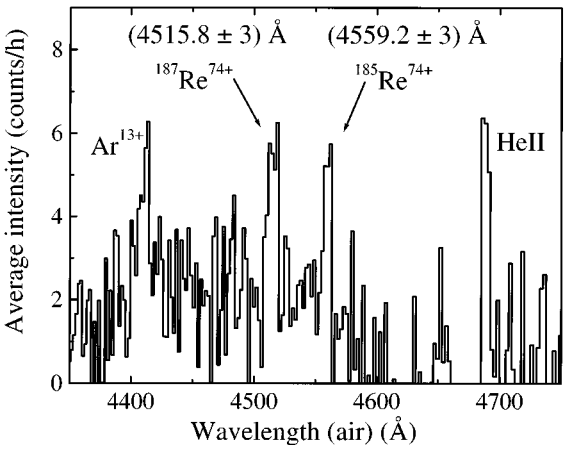

FIG. 2. Spectrum showing the two lines corresponding to the hyperfine transition $F=3$ to $F=2$ of the isotopes ^{187}Re and ^{185}Re in the $1s$ level of hydrogenlike Re^{74+} (air wavelengths).

cal error in the centroid determination of the hyperfine lines. The linear dispersion on this region of the spectrum is 2.185 Å/pixel. The lines show a full width at half maximum (FWHM) of 5 Å, corresponding to roughly 2.3 pixels. Given the small linewidth in terms of number of pixels, we have to assume a possible error of ± 1 pixel additionally to the statistical and calibration errors. We estimate the total uncertainty in the wavelength determination at ± 3 Å, or 1.8 meV.

E. Results

Twenty days of observation were necessary to obtain appropriate signal-to-noise ratios for the wavelength determination of the hyperfine lines. The spectrum acquired is displayed in Fig. 2.

To exclude the possibility that the lines were emitted by a Re ion with a lower charge state, the experiment was repeated, but making sure that no H-like Re^{74+} could be produced, while keeping the other charge states in the trap essentially unchanged. This was done by lowering the beam energy below the ionization potential of Re-like Re^{73+}, so that no Re^{74+} could be produced.

Unfortunately, the level of background in the optical region during these runs was very high, and the expected signal-to-noise ratio was degraded. Beam instabilities, which can occur at a rate of several per hour, evaporated gases from the cryogenic walls, creating line radiation and bursts of light. The signal count rate in the ^{187}Re line was never better than 40 counts per hour, integrating the total linewidth. In the ^{185}Re line the rate was not higher than 24 counts per hour. Very small fluctuations in the background level made it therefore impossible to obtain a better baseline. The 900 spectra collected during the measurement period were analyzed in batches of 100 spectra, every batch with its corresponding set of observation with and without hydrogenic Re. The background baseline shows a time dependence, depending on the ultrahigh vacuum conditions of the machine, especially after wavelength calibration runs using neutral gas injection.

We disregarded spectra showing excessive noise. The criterion used for rejection was the standard deviation of the signal from zero over the full spectral range. Only the spectra showing the smallest deviations from the baseline were taken, since the expected total signal is very small and larger deviations in any region of the spectrum are an indication of beam instabilities. The presence of the Ar^{13+} line at 4413 Å and of the He II at 4686 Å is due to the background variations mentioned before; those lines appear with various intensities in runs with and without Re injection. Since they are identified unambiguously, they are not assigned to Re. The two features at (4515.8 ± 3) Å and (4559.2 ± 3) Å (air wavelength) are identified as the $1s$ level hfs transitions of the two natural isotopes of that element. The two rhenium hyperfine transitions were never observed without Re injection or at energies below the He-like ionization potential. Their relative intensities are consistent with the isotopic abundances for natural rhenium. The corresponding vacuum wavelengths and transition energies are (4517.0 ± 3) Å, (2.7450 ± 0.0018) eV and (4560.4 ± 3) Å, (2.7190 ± 0.0018) eV, respectively. Table I summarizes these results and the results from other related experiments.

TABLE I. Results from measurements of the hfs splitting of the $1s$ level of hydrogenic ions.

Ion	Experimental hfs splitting (eV)	
$^{165}Ho^{66+}$	2.1645(6)	(Ref. [28])
$^{185}Re^{74+}$	2.7190(18)	(this work)
$^{187}Re^{74+}$	2.7450(18)	(this work)
$^{209}Bi^{82+}$	5.0840(8)	(Ref. [27])

IV. DETERMINATION OF THE MAGNETIZATION RADIUS

The observed hyperfine structure is the result of several different contributions as indicated in Eq. (1) We use here the experimental data to extract the magnetization radius from the Bohr-Weisskopf correction. For this purpose, we need the values of all other parameters contributing to the hyperfine splitting, which are the nuclear magnetic moment, the relativistic correction factor A, the nuclear charge distribution correction factor δ, and the QED radiative corrections $\kappa_{\rm rad}$.

A. Nuclear magnetic moment

The nuclear magnetic moments μ_I are taken from an early measurement of the two naturally occurring isotopes of rhenium ^{185}Re and ^{187}Re, done by nuclear magnetic resonance (NMR) by Alder [42]. It yielded values of $3.1433\mu_N$ and $3.1755\mu_N$ (uncorrected for atomic diamagnetism). The measurement was carried out in an aqueous solution of $NaReO_4$. The calibration was performed by using the resonance of ^{23}Na in a 0.25 molar NaCl aqueous solution with 1 molar $MnSO_4$, and assuming a $2.2158\mu_N$ magnetic moment for that nucleus. The data were acquired at a resonance frequency of 6.4 MHz in a variable magnetic field of around 0.67 T. The resonance linewidth was 0.001 T. In the compilation of Raghavan [43] and in the *Table of Isotopes* [44], a standard atomic diamagnetic correction of 1.0138 applied to the rhenium isotopes, as well as an update of the constants

involved, gives a corrected result of $3.1871(3)\mu_N$ and $3.2197(3)\mu_N$, respectively. Chemical shifts of the NMR frequency, which were not accounted for, and the fact that the electronic structure of the rhenium in that experiment was not that of a free atom, but a chemically bound Re^{7+}, i.e., Re(VII), could, however, have introduced a systematic error in that measurement. We quote the experimental uncertainty in μ_I as given above, that is, 0.0094%. This gives, together with the wavelength determination uncertainty (0.067%), a total experimental uncertainty of 0.076% in the determination of the $1s$ level hfs splitting energy, or 3.3% on the determination of ε.

B. Nuclear charge distribution

Using the above-mentioned value for the nuclear magnetic moment $\mu_I = 3.1871(3)$ nm, the nonrelativistic value for the hfs splitting of ^{185}Re obtained from Eq. (1) is 1.6977 eV. The values for ^{187}Re scale directly with the nuclear magnetic moment. We take the relativistic correction factor $A = 1.7731$ from the tabulation by Pyykkö [37]. It changes the value of the hfs splitting (^{185}Re) to 3.0103 eV for a point charge distribution. The value is reduced by the extension of the nuclear charge distribution. Shabaev [30], using a series expansion of the electronic wave function for a homogeneous nuclear charge distribution with a radius R_0 given by $R_0^2 = 5/3\langle r_c^2\rangle$ [$\langle r_c^2\rangle^{1/2} = 5.351(50)$ from Ref. [45]], finds a correction factor $\delta = 0.0698$ and obtains 2.80002 eV. We use instead a direct numerical solution of the electronic wave function, and find for the same charge distribution a slightly smaller hfs splitting of 2.7963 eV, corresponding to a δ of 0.0711. The discrepancy between our results and those of Shabaev is found to grow with Z [39], and is probably due to omitted higher order terms in the series expansion.

The above value for $\langle r_c^2\rangle^{1/2} = 5.351(50)$ fm was taken from Johnson and Soff [45], who use the relation $\langle r_c^2\rangle^{1/2} = (0.836A^{1/3} + 0.570 \pm 0.05)$ fm in the absence of experimental data. However, a more accurate value $\langle r_c^2\rangle^{1/2} = 5.39(1)$ fm can be obtained by interpolating experimental results for the element with $Z = 74$ (W) and 76 (Os). The values for the isotopes of those elements with 110 neutrons were taken from a recent compilation by Nadjakov [46], and agree well with data given by Fricke [47]. The skin thickness parameter is 0.523 fm, interpolated again from Refs. [46, 47]. These data are also consistent with the values found in Refs. [48, 49].

Using a Fermi charge distribution with a charge radius of $\langle r_c^2\rangle = 5.39(1)$ fm, and a thickness parameter $a = 0.523(10)$ fm, we obtain a hfs splitting of 2.7965 eV (corresponding to a charge distribution correction $\delta = 0.0710$). We have chosen this Fermi distribution as a reference, and analyzed changes in the hyperfine splitting resulting from small changes in the charge distribution. With these data, the coefficients of Eq. (3) are found to be $x_r = -0.000\,925\ \mathrm{fm}^{-2}$, and $x_a = 0.001\,73\ \mathrm{fm}^{-2}$ [39]. A variation of the charge radius corresponding to its estimated uncertainty results in a relative change in the calculated hfs splitting of $\pm 10^{-4}$, and an uncertainty of $\pm 0.4\%$ in the value of ε due to systematic uncertainties in the charge distribution. For thickness parameters in the range $0.513 < a < 0.533$ fm the relative error in the hfs splitting obtained using this approximation is $\pm 2 \times 10^{-5}$. This gives a total $\pm 1.2 \times 10^{-4}$ relative error in the hfs splitting due to systematic uncertainties in the nuclear charge distribution or $\pm 0.5\%$ of the value of ε. Assuming the same charge distribution for the two isotopes leads to a BW effect that is about $(0.29 \pm 1.00)\%$ larger for ^{187}Re than for ^{185}Re.

TABLE II. Bohr-Weisskopf correction ε for H-like ions determined from experiments and comparison with predicted values (first uncertainty from charge distribution and QED, second from μ_I, third from hfs splitting measurement).

Isotope	μ_I (nm)	predicted ε %			experimental ε %
^{165}Ho	4.132(3)[a]		0.86[b]		0.92(3)(12)(3)
^{185}Re	3.1871(3)[a]		1.3[b]		2.233(17)(9)(64)
^{187}Re	3.2197(3)[a]		1.3[b]		2.298(17)(9)(64)
^{209}Bi	4.1103(5)[c]	1.1[b]	1.3[d]	2.1[e]	1.472(20)(12)(15)

[a] μ_I taken from *Table of Isotopes* (Ref. [44]).
[b] Shabaev, using a homogeneous distribution of the magnetic moment coinciding with the charge distribution [30].
[c] μ_I taken from Bastug *et al.* [53].
[d] Labzowski *et al.*, dynamic proton model [51].
[e] Tomaselli *et al.*, dynamically correlated nuclear shell model [52].

C. QED radiative corrections

The two dominant QED corrections have been taken from recently published papers. Based on the calculations of the self-energy correction by Persson *et al.* [31], by interpolating from the given data we obtain a -28.16 meV correction. Blundell *et al.* [50] predict for this correction a very close value of -28.17 meV. For the vacuum polarization, calculations by Schneider *et al.* in Ref. [32] give a VP correction of $+14.88$ meV, giving an estimated total net QED correction for ^{185}Re of -13.3 meV, and -13.4 meV for ^{187}Re. Recent calculations by Sunnergren *et al.* [33] give slightly modified values for the total QED corrections: -10.8 meV, -15.1 meV, -15.2 meV, and -30.3 meV for ^{165}Ho, ^{185}Re, ^{187}Re, and ^{209}Bi, respectively, with eximated uncertainties of 1%. This uncertainty contributes 0.2% to the systematic error in the determination of ε.

Note added in proof. Recently, calculations for the QED corrections for H-like ions were performed by P. Sunnergren *et al.*, who have kindly allowed us to use and quote their results in this paper. The numbers in the tables have been slightly revised to account for these values.

D. Determination of ε

For the reference Fermi charge distribution [$\langle r_c^2\rangle = 5.39(1)$ fm, $a = 0.523$ fm] we obtain after subtracting QED effects an experimental value of the Bohr-Weisskopf correction of $\varepsilon = 2.233(17)(9)(64)\%$, where the first uncertainty results from the uncertainty in the charge distribution (radius and skin thickness) and in the QED corrections, the second from the uncertainty in the value of μ_I, and the third from the experimental error in the wavelength determination of the hfs transition. For ^{187}Re we obtain $\varepsilon = 2.298(17)(9)(64)\%$.

TABLE III. The parameters a and b in Eq. (4) describing the sensitivity to the nuclear magnetization distribution (from [39]).

Element	a_2 (10^{-4} fm^{-2})	a_4 (10^{-6} fm^{-4})	a_6 (10^{-9} fm^{-6})	b_2 (10^{-3} fm^{-2})	b_4 (10^{-6} fm^{-4})	b_6 (10^{-9} fm^{-6})
Ho	4.8	−2.0	4.6	2.9	−0.9	1.7
Re	6.2	−2.5	5.0	3.7	−1.1	2.1
Bi	8.0	−3.2	7.1	4.8	−1.4	2.6

We also analyze the published hfs splitting data for H-like Ho^{66+} [28] and Bi^{82+} [27] in terms of the BW correction. We compare our results with some theoretical predictions in Table II.

The prediction of Ref. [30], where a magnetic distribution with $\langle r_m^2\rangle \approx \langle r_c^2\rangle$ is used, is a BW correction of 1.3% for Re. This calculation disagrees with our experimental result by a factor of almost 2, well beyond the experimental and systematic uncertainties. One might expect that the magnetic moment would essentially follow the unpaired proton, and should thus be more extended than the charge distribution. Indeed, if instead of being uniformly distributed the magnetization is concentrated mainly on the surface, the BW correction to the hyperfine structure increases roughly by (5/3), giving a 2.2% Bohr-Weisskopf effect.

The experimental ε value can be used to extract radii for the magnetic distribution, since the result is somewhat model independent—the correction ε is determined mainly by the value for $\langle r_m^2\rangle$. By performing calculations for a number of different distributions, the a and b parameters in Eq. (4) can be determined [39], giving the values shown in Table III. These parameters can then be used to find the values for the magnetization radius $\langle r_m^2\rangle^{1/2}$, which reproduces the observed values (assuming that all contributions to the nuclear magnetic moment follow the same distribution). We evaluate the results for three models, where the nuclear magnetization is distributed on a shell, a homogeneous distribution and, finally, a Fermi distribution of the magnetization. A summary of these results is shown in Table IV.

The values for the $\langle r_m^2\rangle^{1/2}$ inferred by the three models differ from each other by no more than 0.2 fm. Given these model-dependent theoretical uncertainties, we present the final results for the magnetization radii with three uncertainties: the first uncertainty relates to the magnetization model dependence, the second to the parametrization of the nuclear charge distribution, and QED calculations, and the third to the experimental error bars from μ_I and wavelength measurement. We obtain thus for ^{185}Re $\langle r_m^2\rangle^{1/2} = 7.57(12)(4)(16)$ fm and for ^{187}Re $\langle r_m^2\rangle^{1/2} = 7.69(12)(4)(16)$ fm.

Analyzing the data from Ref. [28] for ^{165}Ho in the same way we find $\langle r_m^2\rangle^{1/2} = 5.35(4)(9)(43)$ fm. This value of $\langle r_m^2\rangle^{1/2}$ has to be compared with a nuclear charge radius of $\langle r_c^2\rangle^{1/2} = 5.21(1)$ fm (see Refs. [45–49]). We thus find that the Ho magnetization distribution is roughly similar to the charge distribution, although this result has a large uncertainty due to the error bar of the μ_I value [44]. Similarly, we take the ^{209}Bi results from Ref. [27] and find $\langle r_m^2\rangle^{1/2} = 6.59(4)(5)(7)$ fm, as compared with $\langle r_c^2\rangle^{1/2} = 5.519(2)$ fm (see Refs. [45–49]). The Bi magnetization is described by a radius about 20% larger. The Bi Bohr-Weisskopf corrections calculated in earlier work, 1.1% (Ref. [30]), 1.3% (Ref. [51]), and 2.1% (Ref. [52]), correspond to radii of 5.6, 6.1, and 7.8 fm, respectively.

V. CONCLUSION

We presented a measurement of the hyperfine splitting of the 1s level of hydrogenic ions of the two natural isotopes of rhenium. By using available data on the nuclear magnetic moment, nuclear charge radius, and QED we determine a Bohr-Weisskopf correction of the hfs of the 1s level of the H-like Re^{74+} ions of $\varepsilon(^{185}\text{Re}) = 2.233(17)(73)\%$ and $\varepsilon(\text{Re}^{187}) = 2.298(17)(73)\%$, where the first uncertainty arises from the linear addition of the uncertainties in the charge distribution and QED effects, and the second from the addition of the uncertainties in μ_I and our experimental error bars.

From the measured values for ε and using several models for the nuclear magnetization, we infer the radius for the distribution of the nuclear magnetization and find $\langle r_m^2\rangle^{1/2}(^{185}\text{Re}) = 7.57(12)(4)(16)$ fm and $\langle r_m^2\rangle^{1/2}(^{187}\text{Re}) = 7.69(12)(4)(16)$ fm, where the quoted uncertainties corre-

TABLE IV. Measured Bohr-Weisskopf correction ε and inferred magnetization radii $\langle r_m^2\rangle^{1/2}$. Error budget of experimental results and model dependence of radii. The uncertainty in the first parentheses arises from the linear addition of the uncertainties in the charge distribution and QED effects, and the second from the addition of the uncertainties in μ_I and our experimental error bars.

	Uncertainties in ε (10^{-2})				ε	$\langle r_m^2\rangle^{1/2}$ (fm)		
Isotope	QED	r_c	μ_I	λ	(10^{-2})	Shell	Homogeneous	Fermi
^{185}Re	0.005	0.012	0.009	0.064	2.233(17)(73)	7.45(4)(15)	7.61(4)(16)	7.64(4)(16)
^{187}Re	0.005	0.012	0.009	0.064	2.298(17)(73)	7.57(4)(15)	7.73(4)(16)	7.76(4)(16)

spond to (a) theoretical model dependence; (b) (charge distribution)+QED; and (c) wavelength and nuclear magnetic moment determination, respectively. These results clearly indicate that the radius of the nuclear magnetization distribution is larger than the nuclear charge radius by a factor 1.40(6) and 1.43(6) for ^{185}Re and ^{187}Re, respectively. They also show the possibilities of hfs measurements of H-like ions to obtain the most precise data on the magnetic structure of the nucleus among the methods now available. The results for Re favor models where the nuclear magnetization appears mainly in an outer shell. Knowledge of various nuclear distributions is of importance for several experiments. The atomic PNC, e.g., depends on a neutron distribution that has not been determined by laboratory experiments. These data are needed for refining atomic structure calculations used to calibrate PNC experiments. If the distribution of a possible *P* and *T* violating nuclear electric dipole moment can be approximated by the distribution of the magnetic dipole moment, the ability for precise determination of the difference $\langle r_c^2\rangle - \langle r_m^2\rangle$ will be of importance for the interpretation of the limits for atomic *P* and *T* violation [19,20]. We hope that the availability of accurate values will stimulate nuclear structure calculations predicting these distributions.

ACKNOWLEDGMENTS

We are thankful for helpful discussions with Thomas Kühl and Jonathan Sapirstein. This work was in part supported by the Office of Basic Energy Sciences and was performed under the auspices of the U.S. Department of Energy by Lawrence Livermore National Laboratory under Contract No. W-7405-ENG-48. Financial support was also provided by the Swedish Natural Science Research Council, NFR (A-M.M.-P. and M.G.H.G.).

[1] E. Fermi, Z. Phys. **60**, 320 (1930).
[2] D. A. Jackson, Proc. R. Soc. London **121**, 432 (1928).
[3] H. Schüler, Naturwissenschaften **16**, 512 (1928).
[4] J. E. Rosenthal and G. Breit, Phys. Rev. **41**, 459 (1932).
[5] A. Bohr and V. F. Weisskopf, Phys. Rev. **77**, 94 (1950).
[6] A. Bohr, Phys. Rev. **81**, 331 (1951).
[7] R. J. Gould, Astrophys. J. **423**, 522 (1994).
[8] S. Büttgenbach, Hyperfine Interact. **20**, 1 (1984).
[9] E. N. Fortson, Y. Pang, and L. Wilets, Phys. Rev. Lett. **65**, 2857 (1990).
[10] C. S. Wood, S. C. Bennett, D. Cho, B. P. Masterson, J. L. Roberts, C. E. Tanner, and C. E. Wiemann, Science **275**, 1759 (1997).
[11] N. H. Edwards, S. J. Phipp, P. E. G. Baird, and S. Nakayama, Phys. Rev. Lett. **74**, 2654 (1995).
[12] P. A. Vetter, D. M. Meekhof, P. K. Majumder, S. K. Lamoreaux, and E. N. Fortson, Phys. Rev. Lett. **74**, 2658 (1995).
[13] B. Q. Chen and P. Vogel, Phys. Rev. C **48**, 1392 (1993).
[14] A. C. Hartley, E. Lindroth, and A.-M. Mårtensson-Pendrill, J. Phys. B **23**, 3417 (1990).
[15] J. L. Rosner, Phys. Rev. D **53**, 2724 (1996).
[16] P. G. H. Sandars, J. Phys. B **23**, L655 (1990).
[17] E. R. Boston and P. G. H. Sandars, J. Phys. B **23**, 2663 (1990).
[18] E. A. Hinds and P. G. H. Sandars, Phys. Rev. A **21**, 471 (1980); **21**, 480 (1980).
[19] A.-M. Mårtensson-Pendrill, in *Methods in Computational Chemistry 5*, edited by S. Wilson (Plenum, New York, 1992).
[20] K. Abdullah, C. Carlberg, E. D. Commins, H. Gould, and S. B. Ross, Phys. Rev. Lett. **65**, 2347 (1990).
[21] S. A. Murthy, D. Krause, Jr., L. Li, and L. R. Hunter, Phys. Rev. Lett. **63**, 965 (1989); L. R. Hunter, Science **252**, 73 (1991).
[22] B. E. Sauer, J. Wang, and E. A. Hinds, Phys. Rev. Lett. **74**, 1554 (1996).
[23] R. Winston, Phys. Rev. **129**, 2766 (1963).
[24] G. L. Borchert, P. G. Hansen, B. Jonson, H. L. Ravn, Q. W. B. Schult, P. Tidemand-Petersson, and the ISOLDE Collaboration, Phys. Lett. A **63**, 15 (1977).
[25] R. Engfer, H. Schneuwly, J. L. Vuilleumier, H. K. Walter, and A. Zehnder, At. Data Nucl. Data Tables **14**, 509 (1974).
[26] L. Essen, R. W. Donaldson, M. J. Bangham, and E. G. Hope, Nature (London) **229**, 110 (1971).
[27] I. Klaft, S. Borneis, T. Engel, B. Fricke, R. Grieser, G. Huber, T. Kühl, D. Marx, R. Neumann, S. Schröder, P. Seelig, and L. Völker, Phys. Rev. Lett. **73**, 2425 (1994).
[28] J. R. Crespo López-Urrutia, P. Beiersdorfer, D. W. Savin, and K. Widmann, Phys. Rev. Lett. **77**, 826 (1996).
[29] P. Beiersdorfer, A. Osterheld, J. Scofield, J. R. Crespo López-Urrutia, and K. Widmann, Phys. Rev. Lett. (to be published).
[30] V. M. Shabaev, J. Phys. B **27**, 5825 (1994).
[31] H. Persson, S. M. Schneider, W. Greiner, G. Soff, and I. Lindgren, Phys. Rev. Lett. **76**, 1433 (1996).
[32] S. M. Schneider, W. Greiner, and G. Soff, Phys. Rev. A **50**, 118 (1994); S. M. Schneider (private communication).
[33] P. Sunnergren *et al.* (private communication).
[34] G. Breit, Phys. Rev. **35**, 1147 (1930).
[35] G. Racah, Nuovo Cimento **8**, 178 (1931).
[36] H. Kopfermann, in *Nuclear Moments* (Academic, New York, 1958).
[37] P. Pyykkö, E. Pajanne, and Mitio Inokuti, Int. J. Quantum Chem. **VII**, 785 (1973).
[38] H. H. Stroke, R. J. Blin-Stoyle, and V. Jaccarino, Phys. Rev. **123**, 1326 (1961).
[39] M. G. H. Gustavsson and A.-M. Mårtensson-Pendrill, Adv. Quantum Chem. (to be published).
[40] A.-M. Mårtensson-Pendrill, Phys. Rev. Lett. **74**, 2184 (1995).
[41] A. Bohr and B. R. Mottelson, in *Nuclear Structure, I: Single-Particle Motion* (Benjamin, New York, 1969).
[42] F. Alder and F. C. Yu, Phys. Rev. **82**, L105 (1951).
[43] P. Raghavan, At. Data Nucl. Data Tables **42**, 189 (1987).
[44] R. Firestone *et al.*, in *Table of Isotopes*, 8th ed., edited by V. S. Shirley (Wiley, New York, 1996), Appendix E.
[45] W. R. Johnson and G. Soff, At. Data Nucl. Data Tables **33**, 405 (1985).
[46] E. G. Nadjakov, K. P. Marinova, and Y. P. Gangrsky, At. Data Nucl. Data Tables **56**, 133 (1994).

[47] G. Fricke *et al.* At. Data Nucl. Data Tables **60**, 177 (1995).
[48] C. W. de Jager, H. de Vries, and C. de Vries, At. Data Nucl. Data Tables **14**, 485 (1974).
[49] H. de Vries, C. W. de Jager, and C. de Vries, At. Data Nucl. Data Tables **36**, 495 (1987).
[50] S. A. Blundell, K. T. Cheng, and J. Sapirstein, Phys. Rev. A **55**, 1857 (1997).
[51] N. Labzowsky, W. R. Johnson, G. Soff, and S. M. Schneider, Phys. Rev. A **51**, 4597 (1995).
[52] M. Tomaselli, S. M. Schneider, E. Kankeleit, and T. Kühl, Phys. Rev. C **51**, 2989 (1995).
[53] T. Bastug, B. Fricke, M. Finkbeiner, and W. R. Johnson, Z. Phys. D **37**, 281 (1996).